JOURNAL OF SOLID STATE CHEMISTRY **141,** 599–603 (1998)
ARTICLE NO. SC988026

LETTER TO THE EDITOR

$Sr_3Mn_2O_7$: Mn^{4+} Parent Compound of the $n = 2$ Layered CMR Manganites

J. F. Mitchell, J. E. Millburn, M. Medarde, S. Short, and J. D. Jorgensen

Materials Science Division, Argonne National Laboratory, Argonne, Illinois 60439

and

M. T. Fernández-Díaz

Institut Laue-Langevin, B.P. 156, 30056 Grenoble Cedex 9, France

Communicated by H.-C. zur Loye, August 3, 1998; accepted August 18, 1998

We report the crystal and magnetic structures of the bilayer Ruddlesden–Popper phase $Sr_3Mn_2O_{7-\delta}$ ($\delta = 0.0$, 0.45). The $\delta = 0.45$ compound exhibits a large number of oxygen vacancies disordered in the MnO_2 planes and is a nonmagnetic insulator. $Sr_3Mn_2O_{7.0}$ ($\delta = 0$) in an antiferromagnetic insulator whose magnetic structure is analogous to that of the related $SrMnO_3$ perovskite. The stoichiometric layered material has a small distortion of its exclusively $Mn^{4+}O_6$ octahedra as a result of steric influence of the surrounding cations. Thus, it provides a baseline for structural distortions related to electronic and/or magnetic transitions in doped materials.

I. INTRODUCTION

Mixed-valent manganite perovskites have received substantial attention in recent years, specifically because of colossal magnetoresistance (CMR) and more generally because of their strong coupling among lattice, spin, and charge degrees of freedom (1–3). Layered CMR materials of the formula $La_{2-2x}Sr_{1+2x}Mn_2O_7$ have also garnered attention due to their potential as model systems for low-dimensional physics (4–7) and because they exhibit low-field magnetoresistance substantially better than their perovskite relatives (8).

We report the synthesis and full structural and magnetic characterization of the Mn^{4+} end member of the $n = 2$ Ruddlesden–Popper (R–P) series, $Sr_3Mn_2O_{7-\delta}$ ($\delta = 0.45$, 0.0). The highly oxygen-deficient $Sr_3Mn_2O_{6.55}$ formally contains Mn^{3+} and Mn^{4+}, but is "doped" in a considerably different fashion than the La-substituted materials. The result is a mixed-valent compound whose differing coordination polyhedra localize the e_g electron. Structural distortions observed in the $\delta = 0$ compound arise solely from the steric influence of the tetragonal lattice. As such, it provides a "baseline" for models of doped materials in which octahedral distortions may influence magnetic and/or electronic behavior.

II. EXPERIMENTAL

Synthesis of the double-layer R–P phase $Sr_3Mn_2O_7$ was first reported by Mizutani *et al.* (9). The compound is metastable below 1600°C and must be cooled rapidly to below 1000°C to prevent decomposition to α-Sr_2MnO_4 and $Sr_4Mn_3O_{10}$, neither of which is a layered R–P phase. Mizutani *et al.* slow-cooled their sample from 1000°C and indexed its powder X-ray pattern on a tetragonal cell, *I*4/*mmm*, with lattice parameters given in Table 1. No further characterization of this compound has been reported in the literature.

We synthesized $Sr_3Mn_2O_7$ by firing a stoichiometric mixture of $SrCO_3$ and MnO_2 at 1650°C for 12 h. The pelletized sample was quenched directly from synthesis temperature into dry ice. The resulting sample was dark brown and poorly sintered. An approximately 50-mg portion of this as-made sample was rapidly heated on a TGA balance to 400°C in flowing O_2, held at this temperature until no further weight change was observed, then quickly cooled to room temperature. Annealing the oxygenated sample in ultrahigh purity Ar at 400–500°C failed to reverse the

0022-4596/98 $25.00

oxygen absorption. Samples suitable for neutron diffraction were prepared by annealing 3–5 g of quenched material in 100% O_2 at 400°C for 6 h.

Time-of-flight (TOF) neutron powder diffraction on both as-made and O_2-annealed samples was performed as a function of temperature on the Special Environment Powder Diffractometer (SEPD) at Argonne National Laboratory's Intense Pulsed Neutron Source (IPNS). An additional room temperature powder diffraction pattern of the O_2-annealed sample was recorded on the high-resolution diffractometer D2B (Ge (335), $\lambda = 1.594$ Å) at the Institut Laue-Langevin. All data were analyzed with the Rietveld program FullProf (10). A small concentration of $SrMnO_3$ not observed in the X-ray patterns was included in the refinements as a second phase.

III. RESULTS AND DISCUSSION

Powder X-ray diffraction of the as-made sample revealed a single-phase material qualitatively like that prepared by Mizutani *et al.* (9). However, the different synthesis procedure resulted in a considerably different compound characterized by lattice constants larger than those reported by Mizutani *et al.* (see Table 1). This larger cell volume can be understood by considering a substantial concentration of Mn^{3+} in what was intended to be a nominally Mn^{4+} compound. The only plausible way of generating Mn^{3+} in $Sr_3Mn_2O_7$ is by the formation of oxygen vacancies, and the TGA results of Fig. 1 corroborate this hypothesis. Within 3 h at 400°C in pure O_2 the weight gain has saturated. Assuming that the endpoint compound is stoichiometric (i.e., $Sr_3Mn_2O_{7.0}$), then the as-made material can be formulated as $Sr_3Mn_2O_{6.56}$, i.e., $\delta = 0.44$. Independent confirmation of these oxygen contents was provided by iodometric titration, which gave values for δ of $\delta = 0.45 \pm 0.01$ and $\delta = 0.02 \pm 0.01$ for the as-made and oxygenated samples, respectively. We believe the procedure of Mizutani *et al.* resulted in oxygen uptake during the slow cool-down from 1000°C, yielding the $\delta = 0.0$ compound.

Neutron diffraction measurements of the $\delta = 0.45$ compound revealed an unusual defect structure with all O vacancies located in the MnO_2 planes (see inset of Fig. 1). A far more common defect structure in $n = 2$ and $n = 3$ R–P phases locates the oxygen vacancy between the MO_2 planes. Examples of such a defect structure include $Sr_3V_2O_{7-\delta}$ (11), $Sr_4V_3O_{10-\delta}$ (12), $Sr_3Fe_2O_{7-\delta}$ (13), $Sr_3Co_2O_{6.06}$ (14), and $La_{1.6}Sr_{0.4}CaCu_2O_6$ (15). In-plane defects have been found in $n = 1$ R–P nickelates, often with ordered superlattices (16). Importantly, an arrangement of in-plane oxygen defects has been reported by Leonwicz *et al.* in the $n = 1$ R–P compound $Ca_2MnO_{3.5}$ (17). This compound contains exclusively Mn^{3+} and forms an ordered defect structure of vertex-linked square pyramids. By analogy with $Ca_2MnO_{3.5}$, we may associate the octahedral sites of $Sr_3Mn_2O_{6.55}$ with Mn^{4+} and the square pyramidal sites with Mn^{3+}. The lack of superlattice reflections for $20 \leq T \leq 300$ K indicates that there is no long-range

TABLE 1
Crystal Structure Data from Neutron Powder Diffraction[a]

	$Sr_3Mn_2O_7$ (300 K)[b]	$Sr_3Mn_2O_{7-\delta}$ (300 K, quenched)	$Sr_3Mn_2O_{7.0}$ (300 K, O_2 annealed)	$Sr_3Mn_2O_{7.0}$ (8 K, O_2 annealed)[c]	$La_{1.2}Sr_{1.8}Mn_2O_{7-\delta}$ (300 K, Ref. 6)
a (Å)	3.801(1)[d]	3.82812(3)	3.79972(5)	3.78936(4)	3.87416(3)
c (Å)	20.06(1)	20.1042(3)	20.0959(4)	20.0638(4)	20.1169(3)
Mn z[g]	—	0.09719	0.09707	0.09705	—
O(2) z	—	0.19166	0.19192	0.19181	—
O(3) z	—	0.09535	0.09537	0.09558	—
Sr(2) z	—	0.31540	0.31646	0.31656	—
Mn–O(1) (Å)	—	1.954(3)	1.951(4)	1.947(4)	1.942(4)
Mn–O(2) (Å)	—	1.899(4)	1.906(6)	1.901(5)	1.994(5)
Mn–O(3) (Å)	—	1.91406(6)	1.89986(1)	1.89468(1)	1.93733(7)
D[e]	—	—[f]	1.015	1.016	1.016
δ	—	0.45(2)	0.00[h]	0.00[h]	0.06(5)
$\mu(\mu_B/\text{Mn})$	—	—	—	2.31(7)	—

[a]Entries in this table are from TOF data taken on SEPD.
[b]Data from Ref. (9).
[c]Refined in magnetic supercell; parameters refer to crystallographic subcell. See text for details.
[d]Numbers in parentheses are esd's.
[e]Distortion coordinate, see text for details.
[f]The defect structure makes computation of D meaningless in this compound.
[g]Positions of atoms in $I4/mmm$ (No. 139) are Mn in 4e, Sr(1) in 2b, Sr(2) in 4e, O(1) in 2a, O(2) in 4e, and O(3) in 8g.
[h]Fixed at full O stoichiometry based on refinement of constant wavelength data measured on D2B.

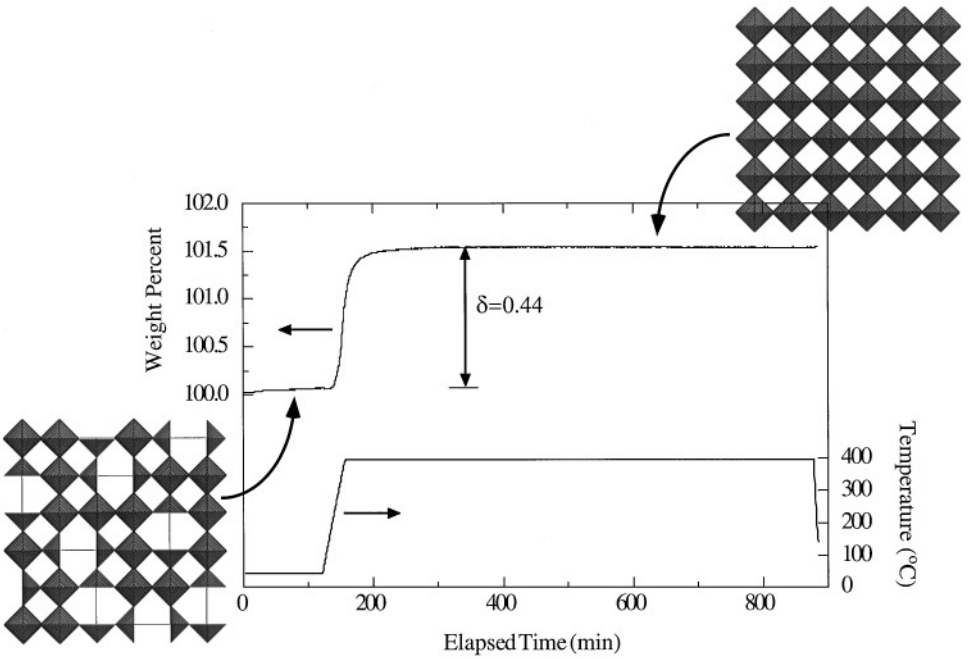

FIG. 1. Thermogravimetric analysis of as-made $Sr_3Mn_2O_{7-\delta}$ in 100% O_2. Insets show schematic of the MnO_2 planes of the as-made and oxygenated samples.

correlation among these coordination polyhedra within the bilayers. In addition, the lack of anisotropic broadening in the diffraction patterns, as seen in microtwinned samples of $La_{2-x}Sr_xNiO_{4-\delta}$ (16), suggests that $Sr_3Mn_2O_{6.55}$ is truly a disordered tetragonal material.

The highly defective structure of $Sr_3Mn_2O_{6.55}$ provides an explanation for the transport and magnetic behavior. Four-probe resistance measurements on a sintered pellet revealed a highly resistive compound between 12 K and room temperature. The insulating behavior may arise from the distinctly different coordination polyhedra trapping the e_g electron on Mn^{3+} (18). Since the defect structure of $Sr_3Mn_2O_{6.55}$ is disordered, the details of the individual Mn–O bond lengths composing the octahedra and square pyramids are undetermined. However, in the ordered defect compound $Ca_2MnO_{3.5}$ mentioned above, the five Mn–O bond lengths are 1.80, 1.93, 1.94 ($\times 2$), and 1.96 Å; the extremely short bond lies in the *a–b* plane. If this geometry is representative of that found in $Sr_3Mn_2O_{6.55}$, then it is reasonable to associate the extreme distortion with localization of the e_g electron on the Mn^{3+} site. As shown by neutron diffraction (and by bulk magnetic susceptibility measurements), $Sr_3Mn_2O_{6.55}$ does not magnetically order above 20 K. The double-exchange ferromagnetism associated with the CMR manganites (19–21) is not expected when the e_g electron is localized. Furthermore, the disordered array of Mn^{3+} and Mn^{4+} sites may frustrate long-range superexchange-mediated magnetic order. It is interesting to speculate that such frustration might be relieved if the vacancies could be ordered.

The fully oxygenated $Sr_3Mn_2O_{7.0}$ compound ($\delta = 0$) has intact MnO_2 sheets containing only $Mn^{4+}O_6$ octahedra. As expected, this material is an antiferromagnetic insulator whose magnetic structure bears strong resemblance to the $SrMnO_{3.0}$ perovskite. Figure 2 shows the results of full profile Rietveld refinements of TOF neutron powder diffraction data taken on a sample of $Sr_3Mn_2O_{7.0}$. Details of the refinement—including corroboration of the oxygen content—are collected in Table 1. As can be seen in Fig. 2, the 8 K diffraction pattern shows magnetic superlattice reflections that can be indexed on a $2a_0 \times 2a_0 \times c_0$ supercell, where a_0 and c_0 are the unit cell dimensions of the paramagnetic phase. The Néel temperature determined by the onset of intensity in the superlattice reflections is $T_N = 160$ K. The refined magnetic structure, shown schematically in Fig. 3, consists of an array of Mn moments aligned parallel to the *c* axis. Each spin is oriented antiparallel to its five neighboring spins, analogous to the G-type antiferromagnetism observed in the perovskite $SrMnO_{3.0}$ ($T_N = 260$ K) (22). The single-layer compound β-Sr_2MnO_4 has a similar spin arrangement in its antiferromagnetic phase ($T_N = 170$ K) (23). The strikingly similar Néel temperatures for the $n = 1$ and $n = 2$ compounds, far below that of the $n = \infty$ perovskite, suggest that T_N is determined largely by interbilayer magnetic interactions. Like cubic $SrMnO_3$ and β-Sr_2MnO_4, $Sr_3Mn_2O_7$ is an insulator resulting from exchange splitting of the occupied t_{2g} orbitals.

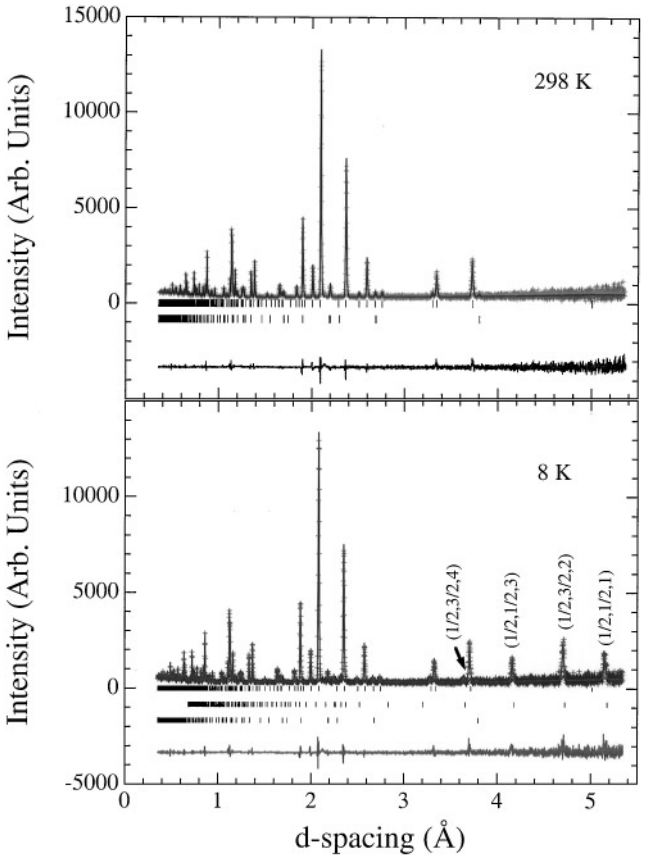

FIG. 2. Results of Rietveld refinement of neutron powder data on $Sr_3Mn_2O_7$ taken at 298 K (top) and 8 K (bottom). (+): Observed; (−): calculated. Difference curves are shown at the bottom of each panel. Vertical lines mark positions of (top to bottom) fundamental reflections for double-layer material, magnetic reflections (bottom panel only), and $SrMnO_3$ impurity phase.

The magnetic ordering, the metal–insulator transition, etc., in the doped $La_{2-2x}Sr_{1+2x}Mn_2O_7$ compounds may correlate sensitively with the Mn–O bond lengths (24, 25). Containing no Jahn–Teller active Mn^{3+} ions, $Sr_3Mn_2O_{7.0}$ serves as a "baseline" for studying such MnO_6 octahedral distortions in the doped materials. The three symmetry-independent Mn–O bond lengths in $Sr_3Mn_2O_{7.0}$ are collected in Table 1. The distortion is rather small but nonzero. In particular, the in-plane Mn–O(3) and out-of-plane Mn–O(2) are quite short, while the Mn–O(1) bond shared between the layers is somewhat longer. Unlike doped materials (6), no substantial change in bond lengths occurs between room temperature and 8 K. The octahedral distortion coordinate, defined as $D = \langle Mn - O_{apical} \rangle / Mn - O_{equatorial}$, is 1.015 at 298 K and increases slightly to 1.016 at 8 K. A comparison to typical values of 1.01–1.04 in the doped materials (6)—where the individual bond lengths are quite different from those in the undoped compound (e.g., see Table 1)—demonstrates two points: (1) Even a compound containing no Jahn–Teller active Mn^{3+} can exhibit a distorted coordination polyhedron arising simply from its steric environment, and (2) caution must be exercised when using a single parameter to characterize the octahedral distortion in these layered materials.

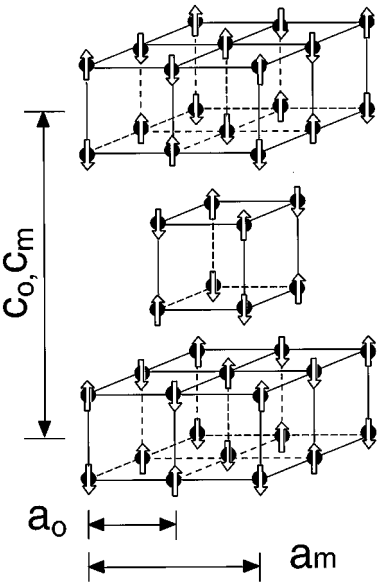

FIG. 3. Magnetic structure of $Sr_3Mn_2O_{7.0}$ at 8 K with crystallographic (a_c, c) and magnetic (a_m, c) unit cells outlined. Arrows represent direction of Mn moment. For clarity, only Mn atoms are shown.

IV. SUMMARY

The $n = 2$ R–P phase $Sr_3Mn_2O_{7-\delta}$ forms with oxygen vacancies in the MnO_2 planes. The resulting mixed-valent compound contains a disordered array of octahedra and square pyramids and is a nonmagnetic insulator. The oxygen vacancies can be irreversibly filled at 400°C to yield stoichiometric $Sr_3Mn_2O_7$, which is an antiferromagnetic insulator. The small octahedral distortions in this latter compound provide a baseline for studying charge–lattice coupling in doped $La_{2-2x}Sr_{1+2x}Mn_2O_7$ CMR materials.

ACKNOWLEDGMENTS

This work was supported by the U.S. Department of Energy, Basic Energy Sciences–Materials Sciences under Contract W-31-109-ENG-38. M.M. acknowledges support of the Swiss National Science Foundation. The authors thank Dr. Richard Osgood, III for magnetic susceptibility measurements and Ms. J. Siewenie for resistivity measurements.

REFERENCES

1. A. Urushibara, Y. Moritomo, T. Arima, A. Asamitsu, G. Kido, and Y. Tokura, *Phys. Rev. B* **51,** 14,103–14,109 (1995).
2. P. G. Radaelli, M. Marezio, H. Y. Hwang, S.-W. Cheong, and B. Batlogg, *Phys. Rev. B* **54,** 8992 (1996).

3. M. R. Ibarra, P. A. Algarabel, C. Marquina, J. Biasco, and J. García, *Phys. Rev. Lett.* **75,** 3541 (1995).
4. D. N. Argyriou, J. F. Mitchell, C. D. Potter, S. D. Bader, R. Kleb, and J. D. Jorgensen, *Phys. Rev. B* **55,** 11,965R (1997).
5. P. D. Battle, D. E. Cox, M. A. Green, J. E. Millburn, L. E. Spring, P. G. Radaelli, M. J. Rosseinsky, and J. F. Vente, *Chem. Mater.* **9,** 1042 (1997).
6. J. F. Mitchell, D. N. Argyriou, J. D. Jorgensen, D. G. Hinks, C. D. Potter, and S. D. Bader, *Phys. Rev. B* **55,** 63 (1996).
7. Y. Moritomo, Y. Tomioka, A. Asamitsu, Y. Tokura, and Y. Matsui, *Phys. Rev. B* **51,** 3297 (1995).
8. Y. Moritomo, A. Asamitsu, H. Kuwahara, and Y. Tokura, *Nature* **380,** 141 (1996).
9. N. Mizutani, A. Kitazawa, O. Nobuyuki, and M. Kato, *J. Chem. Soc.* (*Jpn.*) *Ind. Ed.* **73,** 1097 (1970).
10. J. Rodríguez-Carvajal, *Physica B* **192,** 55 (1993).
11. M. Itoh, M. Shikano, H. Kawaji, and T. Nakamura, *Solid State Comm.* **80,** 545 (1991).
12. W. Gong, J. S. Xue, and J. E. Greedan, *J. Solid State Chem.* **91,** 180 (1991).
13. S. E. Dann, M. T. Weller, and D. B. Currie, *J. Solid State Chem.* **97,** 179 (1992).
14. S. E. Dann and M. T. Weller, *J. Solid State Chem.* **115,** 499 (1995).
15. R. J. Cava, A. Santoro, J. J. Krajewski, R. M. Fleming, J. V. Waszczak, W. F. Peck, Jr., and P. Marsh, *Physica C* **172,** 138 (1990).
16. M. Medarde and J. Rodríguez-Carvajal, *Z. Phys. B* **102,** 307 (1997).
17. M. E. Leonowicz, K. R. Poeppelmeier, and J. M. Longo, *J. Solid State Chem.* **59,** 71 (1985).
18. M. Robin and P. Day, *Adv. Inorg. Chem. Radiochem.* **10,** 247 (1967).
19. P. W. Anderson and H. Hasegawa, *Phys. Rev.* **100,** 675 (1955).
20. P. G. deGennes, *Phys. Rev.* **118,** 141 (1960).
21. J. B. Goodenough, *in* "Magnetism and the Chemical Bond" (F. A. Cotton, Ed.). Wiley, New York, 1963.
22. T. Takeda and S. Ohara, *J. Phys. Soc. Jpn.* **37,** 275 (1974).
23. J.-C. Bouloux, J.-L. Soubeyroux, G. Le Flem, and P. Hagenmuller, *J. Solid State Chem.* **38,** 34 (1981).
24. Y. Moritomo, Y. Mauryama, T. Akimoto, and A. Nakamura, *Phys. Rev. B* **56,** R7057 (1997).
25. S. Ishihara, S. Okamoto and S. Maekawa, *J. Phys. Soc. Jpn.* **66,** 2965 (1997).